Nuclear Instruments and Methods in Physics Research A 1088 (2026) 171538

Contents lists available at ScienceDirect

Nuclear Inst. and Methods in Physics Research, A

journal homepage: www.elsevier.com/locate/nima

Full Length Article

spadRICH: Developing digital analog SiPMs as candidate photodetectors for future RICH detectors[☆]

Rok Dolenec [a,b],[*], Edoardo Charbon [c], Won-Yong Ha [c], Samo Korpar [a,d], Peter Križan [a,b], Rok Pestotnik [a], Andrej Seljak [a], Prabhleen Singh [c], Gregor G. Taylor [c], Claudio Bruschini [c],[**]

[a] Experimental Particle Physics Department, Jožef Stefan Institute, Jamova cesta 39, Ljubljana, 1000, Slovenia
[b] Faculty of Mathematics and Physics, University of Ljubljana, Jadranska ulica 19, Ljubljana, 1000, Slovenia
[c] AQUA Laboratory, École polytechnique fédérale de Lausanne (EPFL), Rue de la Maladière 71, Neuchâtel, 2000, Switzerland
[d] Faculty of Chemistry and Chemical Engineering, University of Maribor, Smetanova ulica 17, Maribor, 2000, Slovenia

ARTICLE INFO

Keywords:
Single photon avalanche diode (SPAD)
Radiation-hard detectors
Cryogenic detectors
Neutron irradiation
Cherenkov detectors (RICH)

ABSTRACT

In the next generation of experiments in high energy particle physics a large increase in beam interaction density will necessitate upgrades of particle detectors. Examples are the Ring imaging Cherenkov detectors (RICH) in the planned upgrades of the LHCb, Belle II and ALICE 3 experiments. The upgraded RICH detectors will need photodetectors capable of detecting rings of Cherenkov photons at high rates of true and background events as well as large background radiation. Silicon photomultipliers (SiPMs) are an attractive photodetector candidate, with the main remaining technological challenge being the resistance to neutron radiation damage — during the whole experiment run time, the photodetectors are expected to receive a fluence of a few 10^{13} 1-MeV neutron equivalent/cm^2. To achieve the targeted radiation tolerance, as well as other RICH detector requirements, dedicated developments and a combination of radiation damage reduction and mitigation techniques, such as cryogenic cooling, are needed. The spadRICH project is developing a CMOS single-photon avalanche diode (SPAD) based photodetector optimized for the application of the planned RICH detectors, with SPADs designed specifically for radiation hardness and cryogenic operation. In this work, we report on dark count rate measurements of SPADs designed by the AQUA Lab in 55 nm BCD technology and 110 nm CMOS image sensor technology, performed down to liquid nitrogen temperatures and for neutron irradiation up to 10^{12} 1-MeV neutron equivalent/cm^2.

1. Introduction

Silicon photomultipliers (SiPMs) are considered as prime photodetector candidates for future ring imaging Cherenkov (RICH) detectors, with their main limitation being the sensitivity to neutron radiation. For example, in the planned LHCb RICH Upgrade II, the photodetectors will have to efficiently detect single photons with timing resolution about 100 ps and limited dark count rate (DCR), even after a total fluence of about 10^{13} 1-MeV neutron equivalent/cm^2 (n$_{eq}$/cm^2). With current technology, this seems barely possible by cooling the SiPMs close to liquid nitrogen temperature [1]. The spadRICH project is developing a digital analog SiPM [2,3] specifically for future RICH detectors. The sensors will be fabricated in standard CMOS technology and optimized for radiation hardness. To guide the design of these sensors, we investigated the performance of existing single photon avalanche diode (SPAD) sensors after neutron irradiation and operating at cryogenic temperatures. We previously reported on the results achieved with 180 nm SPADs [4] produced in standard CMOS technology [5]. Here we present DCR results for SPADs designed by the EPFL AQUA Lab in 55 nm BCD technology [6,7] and 110 nm CMOS image sensor technology [8] irradiated up to 10^{12} n$_{eq}$/cm^2. The low temperature behavior of some of these SPADs, mostly before neutron irradiation, was already investigated in [9].

2. Methods

Table 1 summarizes the design parameters of SPAD samples, which were characterized before and after neutron irradiation performed at the Jožef Stefan Institute TRIGA reactor. Three sets of 55 nm samples were irradiated to fluences of 10^{10} n$_{eq}$/cm^2, 10^{11} n$_{eq}$/cm^2 and

---

[☆] This article is part of a Special issue entitled: ‘RICH2025’ published in Nuclear Inst. and Methods in Physics Research, A.
[*] Corresponding author at: Experimental Particle Physics Department, Jožef Stefan Institute, Jamova cesta 39, Ljubljana, 1000, Slovenia.
[**] Corresponding author.
E-mail addresses: rok.dolenec@ijs.si (R. Dolenec), claudio.bruschini@epfl.ch (C. Bruschini).

https://doi.org/10.1016/j.nima.2026.171538
Received 15 January 2026; Received in revised form 17 March 2026; Accepted 27 March 2026

Table 1
Properties of SPAD samples characterized: technology node in which they are produced, junction type, SPAD diameter (D), breakdown voltage at room temperature (V_{BR}), and temperature coefficient of the breakdown voltage (k_T).

Label	Technology	Junction	D (μm)	V_{BR} (V)	k_T (mV/K)
101	55 nm	P/N	10	31	25
103			12	31	27
331		N/P	8	23	28
335			10	19	19
108005	110 nm	P+/N	5	20	16
115005			5	21	20
115			10	20	15

10^{12} n_{eq}/cm^2. Two sets of 110 nm samples were available and were irradiated in two steps, first to 10^9 n_{eq}/cm^2 and 10^{10} n_{eq}/cm^2, and later to 10^{11} n_{eq}/cm^2 and 10^{12} n_{eq}/cm^2, respectively.

The characterization of SPADs was performed with an experimental setup based on the one presented in [1,9]. The SPAD and front-end amplifier board were placed inside an aluminum box, which was inserted in a dry liquid nitrogen container. Measurements were performed at stabilized temperatures between room (RT) and liquid nitrogen temperature by means of a temperature probe and resistive heaters attached to the aluminum box. The DCR was measured in two ways: using a scaler (Aim-TTi TF930 Universal Counter) and by measuring the inter-pulse arrival times with a custom TDC implemented on Arduino board. The scaler provided accurate measurements of DCR at high rates (> 1 cps), while the TDC enabled also the measurement of lower rates. The DCRs reported here were obtained from scaler measurement for DCR > 100 cps, and from TDC otherwise. The breakdown voltages at each temperature where DCR characterization was performed were determined from a separate calibration measurement for all SPAD samples. We did not observe a change in breakdown voltage even at the highest neutron fluence. All DCR measurements reported were made at temperature-adjusted excess bias voltage of 6 V.

Data was obtained at 11 temperature steps, for up to 30 min per step in order to obtain sufficient statistics in very low DCR cases. Such measurement time placed the lower limit for measurable DCR on the order of 10^{-3} cps. Considering also the settling time between temperature steps, which ranged from 10 min to 30 min, and the time necessary for the breakdown voltage calibration measurement, this meant that at most one sample per day could be characterized.

3. Results and discussion

The DCRs measured at different neutron fluences and temperatures are shown in Figs. 1 and 2. Some data points at lowest temperatures are missing due to disconnects of power or signal lines after continuous temperature cycling. The SPADs survived the lowest irradiation level (10^{10} n_{eq}/cm^2 for 55 nm SPADs and 10^9 n_{eq}/cm^2 for 110 nm SPADs) mostly unaffected, but exhibit large increase in noise (3–5 orders of magnitude at RT) at 10^{12} n_{eq}/cm^2. Since this data was obtained with only a few samples, the results may not accurately represent the statistical effects of irradiation at certain fluences. For example, one sample of SPAD type 115, which was exposed to the fluence of 10^{10} n_{eq}/cm^2, apparently received higher actual damage than the other sample, exposed to 10^{11} n_{eq}/cm^2 (Fig. 2c). Still, most of the results follow the expected trends. First, SPADs with larger volume (diameter) exhibit larger DCR increase with irradiation level (e.g. Fig. 1b vs. a, Fig. 2c vs. b). Second, the smaller technology node seems to perform better, especially the 55 nm N/P junction samples, both of which were unaffected by 10^{11} n_{eq}/cm^2 (Fig. 1c and d), unlike the three samples of 110 nm SPAD, all of which had an increase in DCR at or before this fluence (Fig. 2). Third, cooling improves the DCR performance, with majority of samples recovering at least three orders of magnitude

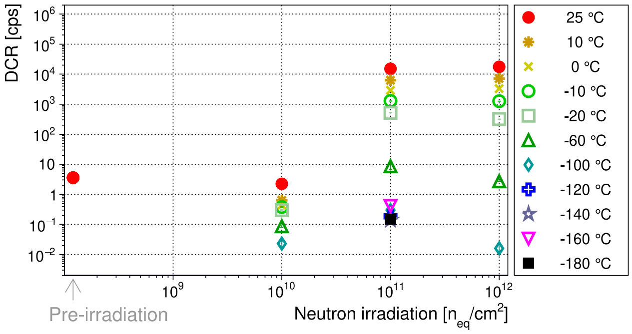

(a) 101 (55 nm, P/N, 10 μm)

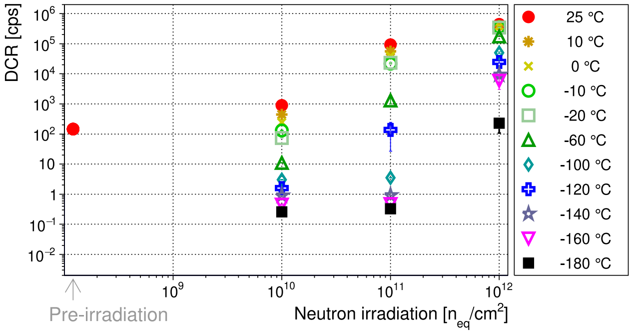

(b) 103 (55 nm, P/N, 12 μm)

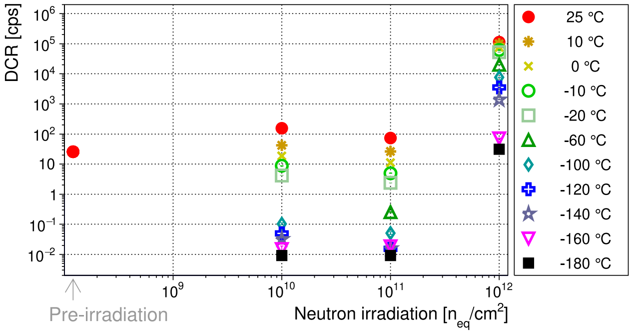

(c) 331 (55 nm, N/P, 8 μm)

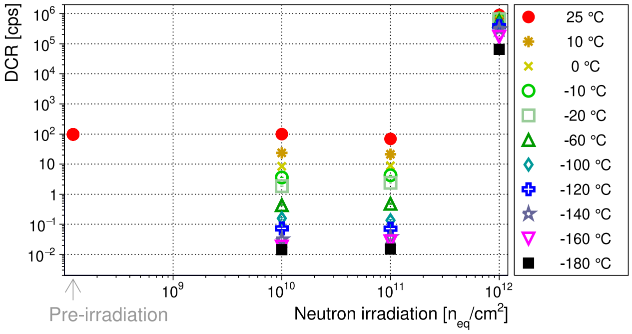

(d) 335 (55 nm, N/P, 10 μm)

Fig. 1. Dark count rates measured at different neutron irradiation levels and temperatures for 55 nm SPAD samples. The leftmost point represents the DCR at RT before irradiation, with its position not corresponding to the scale of the rest of the *x*-axis.

in DCR by −180 °C even at highest fluence (Fig. 1a-c, Fig. 2a and b). On the other hand, two SPADs received especially high damage at 10^{12} n_{eq}/cm^2, as evidenced by the fact that even cooling to the lowest temperature only recovered about one order of magnitude in DCR (Fig.

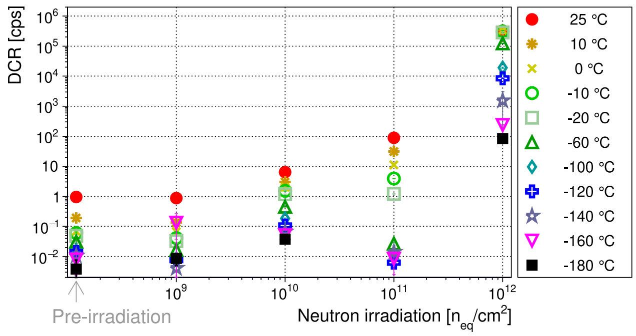

(a) 108005 (110 nm, P+/N, 5 µm)

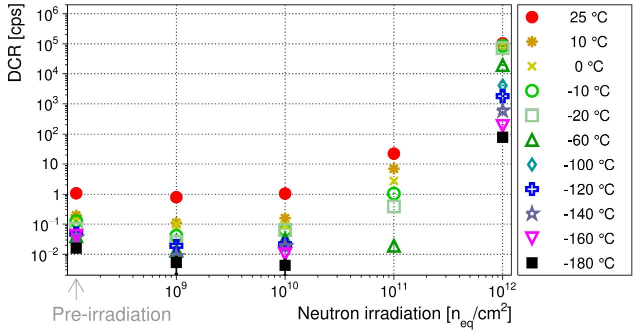

(b) 115005 (110 nm, P+/N, 5 µm)

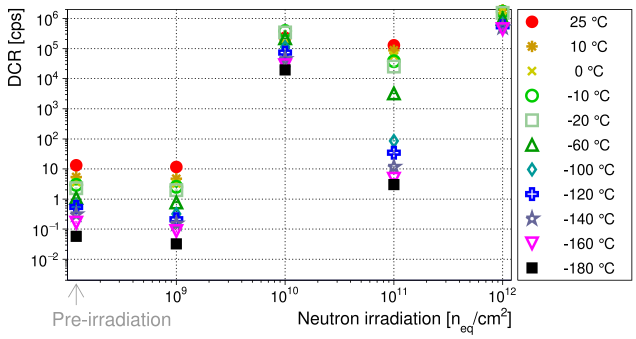

(c) 115 (110 nm, P+/N, 10 µm)

Fig. 2. Dark count rates measured at different neutron irradiation levels and temperatures for 110 nm SPAD samples. The leftmost points represent the DCR values before irradiation, with their position not corresponding to the scale of the rest of the x-axis.

1d and Fig. 2c). These examples illustrate the importance of further improvements needed to achieve radiation hardness in SiPMs up to the required level of about 10^{13} n_{eq}/cm^2, specifically the potential benefits of integrated electronics which would enable switching off the most damaged SPADs.

4. Conclusion

SPADs with different design parameters were characterized in terms of their DCR at different neutron irradiation levels up to 10^{12} n_{eq}/cm^2 and temperatures down to liquid nitrogen temperature. The results obtained with the few samples studied follow the expectations that smaller SPAD active volumes and smaller technology nodes help with radiation hardness. Cooling to −180 °C improved the DCR at the highest irradiation by at least three orders of magnitude for all but a couple of most damaged samples.

Declaration of competing interest

The authors declare the following financial interests/personal relationships which may be considered as potential competing interests: Rok Dolenec reports financial support was provided by Slovenian Research and Innovation Agency. Claudio Bruschini reports financial support was provided by Swiss National Science Foundation. If there are other authors, they declare that they have no known competing financial interests or personal relationships that could have appeared to influence the work reported in this paper.

Acknowledgments

This project has received funding from the Slovenian Research and Innovation Agency (project J1-50009) and the Swiss National Science Foundation, Switzerland (project No 200021E_218853).

References

[1] D. Consuegra Rodríguez, et al., Characterization of neutron-irradiated SiPMs down to liquid nitrogen temperature, Eur. Phys. J. C 84 (2024) 970, http://dx.doi.org/10.1140/epjc/s10052-024-13302-7.

[2] A. Muntean, et al., Towards a fully digital state-of-the-art analog SiPM, in: IEEE NSS/MIC Conference Record, 2017, http://dx.doi.org/10.1109/NSSMIC.2017.8533036.

[3] A. Muntean, et al., Blumino: The First Fully Integrated Analog SiPM With On-Chip Time Conversion, IEEE Trans. Radiat. Plasma Med. Sci 5 (5) (2020) 671–678, http://dx.doi.org/10.1109/TRPMS.2020.3045081.

[4] R. Dolenec, et al., Neutron radiation hardness of single-photon avalanche diodes for future RICH detectors, in: IEEE NSS/MIC Conference Record, 2023, http://dx.doi.org/10.1109/NSSMICRTSD49126.2023.10337871.

[5] F. Gramuglia, et al., A low-noise CMOS SPAD pixel with 12.1 Ps SPTR and 3 Ns dead time, IEEE J. Sel. Top. Quantum Electron. 28 (2) (2022) 3800809, http://dx.doi.org/10.1109/JSTQE.2021.3088216.

[6] F. Gramuglia, et al., Engineering breakdown probability profile for PDP and DCR optimization in a SPAD fabricated in a standard 55 nm BCD process, IEEE J. Sel. Top. Quantum Electron. 28 (2) (2022) 3802410, http://dx.doi.org/10.1109/JSTQE.2021.3114346.

[7] A. Morelle, et al., Deep cryogenic operation of 55 nm CMOS SPADs for quantum information and metrology applications, in: Quantum Information and Measurements VI, 2021, http://dx.doi.org/10.1364/QIM.2021.M2B.7.

[8] M.-J. Lee, et al., A 73% peak PDP single-photon avalanche diode implemented in 110 nm CIS technology with doping compensation, IEEE J. Sel. Top. Quantum Electron. 30 (1) (2024) 3800310, http://dx.doi.org/10.1109/JSTQE.2023.3288674.

[9] R. Dolenec, et al., SiPM and CMOS SPAD characterization at liquid nitrogen temperatures, JINST 20 (2025) P06052, http://dx.doi.org/10.1088/1748-0221/20/06/P06052.